*2009*년 *2*월

박사학위논문

Effect of Nfic disruption during odontoblast differentiation and dentin formation

조선대학교 대학원

치의공학과

김 지 웅

Effect of Nfic disruption during odontoblast differentiation and dentin formation

*2009*년 *2*월 일

조선대학교 대학원

치의공학과

김 지 웅

Effect of Nfic disruption during odontoblast differentiation and dentin formation

지도교수 김 홍 중

이 논문을 치의학 박사학위 신청 논문으로 제출함.

*2008*년 *10*월 일

조선대학교 대학원

치의공학과

김 지 웅

김지웅의 박사학위 논문을 인준함

위원장　조선대학교　교수　윤 창 륙　인

위　원　서울대학교　교수　박 주 철　인

위　원　연세대학교　교수　김 희 진　인

위　원　조선대학교　교수　김 도 경　인

위　원　조선대학교　교수　김 홍 중　인

*2008*년　*12*월　일

조선대학교 대학원

Contents

FIGURE LEGENDS

ABSTRACT

Effect of Nfic disruption during odontoblast differentiation and dentin formation

Kim, Ji-Woong

Advisor : Prof. Kim, Heung-Joong, D.D.S., M.S.D., Ph.D.

Department of Dental Engneering

Graduate School of Chosun University

My previous studies have demonstrated that nuclear factor I-C (*Nfic*) null mice developed short molar roots that contain aberrant odontoblasts and abnormal dentin formation. Based on these findings, I performed studies to elucidate the function of *Nfic* in odontoblasts. Initial studies demonstrated that aberrant odontoblasts become dissociated and trapped in an osteodentin-like mineralized tissue. Abnormal odontoblasts exhibit strong BSP expression, but a decreased level of DSPP expression when compared to wild type odontoblasts. Loss of *Nfic* result in an increase in p-Smad2/3 expression in aberrant odontoblasts and pulp cells in the sub-odontoblastic layer *in viv*o, and primary pulp cells from *Nfic*-deficient mice *in vitro*. Cell proliferation analysis of both cervical loop and ectomesenchymal cells of the *Nfic*-deficient mice revealed significantly decreased proliferative activity compared to normal mice. In addition, *Nfic*-deficient primary pulp cells showed increased expression of p21 and p16, but decreased expression of cyclin D1 and cyclin B1 strongly suggesting a cell growth arrest due to lack of *Nfic* activity. Analysis of apoptotic cells in the sub-odontoblastic layer of the pulp in *Nfic*-deficient mice revealed an increase in apoptotic activity. Further, *Nfic*-deficientprimary pulp

cells exhibited an increasein caspase-8 and -3 activation, while the cleaved form of Bid was hardly detected. These results indicate that the loss of *Nfic* leads to the suppression of odontogenic cell proliferation, differentiation, and induces apoptosis of aberrant odontoblasts during root formation, thereby contributing to the formation of short roots.

I. Introduction

Tooth development is a complex and well-coordinated developmental process that is achieved through a series of reciprocal interactions between dental epithelium and neural crest-derived ectomesenchyme (EM). The dental epithelium gives rise to the outer and inner enamel epithelium from which ameloblasts differentiate, while EM cells differentiate into odontoblasts. The critical roles of several transcription factors and growth factors in crown formation have been relatively well documented (1,2). After completion of crown formation, the inner and outer enamel epithelial cells proliferate and form Hertwig's epithelial root sheath (HERS) that plays a key role in root formation. It is believed, based on information derived from crown development, that HERS induces the differentiation of EM cells from the radicular pulp area into odontoblasts which are responsible for root dentin formation. However, the molecular mechanisms responsible for root development are not well understood (3-5).

The nuclear factor I (*Nfi*) family of transcription/replication factors was first discovered as a family of proteins required for the replication of adenovirus DNA *in vitro* (6). The *Nfi* gene family encodes the site-specific transcription factors essential for the development of a number of organ systems (7). There are four *Nfi* gene family members in vertebrates (*Nfia, Nfib, Nfic,* and *Nfix*) and a single *Nfi* gene in Drosophila melanogaster and Caenorhabditis elegans (Nfi-i) (7,8). The consequences of individual gene disruptions in mice of each of the four *Nfi* genes have been reported. *Nfia*-deficient mice exhibit defects in brain development (9), whereas *Nfib*-deficient mice show defects in lung maturation and brain development (10,11). *Nfix*-deficient mice reveal defects in brain and skeleton development (12). Interestingly, *Nfic*-deficient mice demonstrate aberrant odontoblast differentiation during root formation as well as short root formation and severe incisor defects (13). However, the exact roles of

Nfic in root formation remain unknown.

Transforming growth factor-β (TGF-β), a prominent member of the TGF-β superfamily of ligands including TGF-βs, activins and BMPs, regulates a broad spectrum of biological responses in a variety of cell types (14,15). The exposure of cells to TGF-β1 can trigger a variety of cellular responses including cell growth arrest, differentiation, and apoptosis (16,17). Upon binding of TGF-β1 to the TGF-β receptor II (TGFβ-RII), TGFβ-RIs heterodimerize and are phosphorylated. The activated TGFβ-RI then phosphorylates Smad2 and Smad3 and forms a complex with a common partner, Smad4, which translocates into the nucleus to act as a transcriptional regulator (18). During mouse tooth development, TGF-β1 has been implicated as a key mediator in odontoblast differentiation and dentin mineralization (19). Interestingly, conditional overexpression of TGF-β1 in mouse odontoblasts under the control of the dentin sialophosphoprotein promoter revealed the same phenotypic changes as seen in *Nfic*-deficientmice. These include the presence of aberrant odontoblasts and their entrapment in abnormal dentin (20). Further, treatment with TGF-β1 of immortalized preodontoblastic MDPC-23 cells derived from a mouse molar dental papilla (21, 22) induced the expression of Smad2, Smad3, Smad4, and apoptosis (23).

In the present study, I sought to determine if odontoblasts change phenotypically into osteoblasts in *Nfic*-deficient mice. Further, I investigated whether disruption of the *Nfic* gene causes cell growth arrest and apoptosis of odontoblasts. Finally, I determined the molecular mechanism for cell growth arrest of odontogenic cells and apoptosis in *Nfic*-deficient odontoblasts.

II. Materials & Methods

1. Antibodies.

Antiserum against *Nfic*, DSP, and BSP were produced by immunization of rabbit with the synthetic peptides (NH2)-RPTRPLQTVPLWD-(COOH) (amino acid residues 427~439 of *Nfic*), (NH2)-GNKSIITKESGKLSGS-(COOH) (amino acid residues 372~387 of DSP) and (NH2)-RRIKAEDSEENGVFKYR-(COOH) (amino acid residues 24~40 of BSP). Mouse monoclonal anti-cyclin D1 and rabbit polyclonal anti-p16 were purchased from Cell Signaling Technology. All other antibodies, against TGFβ-RI, p-Smad2/3, p21, cyclin B1, caspase-8, caspase-3, Bid, and cIAP1/2 were purchased from Santa Cruz Biotechnology.

2. Plasmid Constructs.

RNAi *Nfic* plasmid (pLKO.1-*Nfic* shRNA) and control plasmid (pLKO.1) purchased from Open Biosytems. pCH-*Nfic* expression plasmid was provided by Dr. R. M. Gronostajski State University of New York at Buffalo, Buffalo, NY). Full-length Smd2 and Smad3 expression plasmid and a BSP promoter (pGL3LUC-2478~+60) plasmid were kind gifts from Dr. H.-M. Ryoo (Department of Cell and Developmental Biology, School of Dentistry and DRI, Seoul National University, Seoul, Korea). The DSPP promoter (pGL3LUC-791~+54) plasmid was a kind gift from Dr. W.-X. He (Department of Operative Dentistry, Qin Du Stomatological, Xian, China).

3. Tissue preparation and Immunohistochemistry.

Tissue preparation and immunohistochemistry were performed as described previously (24). Briefly, mice were cardiac-perfused with 4% paraformaldehyde-phosphate-buffered saline (PBS), their heads were removed, and then they were decalcified in a 10% ethylenediaminetetra-acetic acid (EDTA, pH 7.4) solution at 4℃ and processed for embedding in paraffin. The deparaffinized sections were immersed in 0.6% H2O2/methanol for 20 min to

quench the endogenous peroxidase activity. They were then pre-incubated with 1% BSA in PBS for 30 min and incubated overnight at 4℃ with rabbit polyclonal DSP, BSP (1:100) or p-Smad2/3 (1:200, Santa Cruz Biotechnology) antibodies. Sections were incubated for 1 h at room temperature with the secondary antibody, and reacted with avidine-biotine-peroxidase complex (Vector Lab) in PBS for 30 min. After color development with 0.05% 3,3′-diaminobenzidine tetrahydrochloride (DAB, Vector Lab), they were counterstained with hematoxylin.

4. Primary pulp cell culture.

Mandibles were removed from 17-days old wild type and *Nfic*-deficient mice. After the incisors were dissected out, they were cracked longitudinally using a 27 G needle on a 1ml syringe. Pulp tissues were removed gently with forceps, cut into several pieces, and placed on 60 mm culture dishes (Nunc). The explants were weighed down with a sterile cover glass and cultured in Dulbecco's modified Eagle's medium (DMEM, Gibco BRL) supplemented with 100 IU/ml penicillin, 100 ㎍/ml streptomycin (Gibco BRL) and 10% fetal bovine serum (FBS, Gibco BRL). The cells were cultured at 37°C in a humidified atmosphere containing 5% CO2 and cells at passage 2 were used in the experiments.

5. BrdU staining for cell proliferation.

Proliferatingcells were detected immunohistochemically after i.p. injection of 5′-bromo-2′-deoxyuridine (BrdU, 50 mg/kg body wt, Sigma-Aldrich). Mice were sacrificed at 4 h after BrdU injection, and their heads were removed and processed for embedding in paraffin as described above. BrdU-labeled cells in 5-㎛ thick sections were then identified using a BrdU staining kit (Zymed Laboratory) according to the manufacturer's instruction, and counterstained with hematoxylin. The labeling indexes for BrdU-immunopositive cervical loop and EM cells were obtained.

6. TUNEL POD staining.

Apoptotic cells were detected in paraffin sections using a terminal deoxynucleotidyl transferase-mediated dUTP nick end labeling (TUNEL) kit (In Situ Cell Death Detection Kit, POD) according to the manufacture's instruction (Roche Molecular Biochemicals). The endogenous peroxidase within the tissue sections was inactivated by incubation for 10 min in 3% H2O2before enzymatic labeling. TUNEL POD staining was achieved by incubation with DAB after enzymatic labeling and sections were counter-stained with methyl green.

7. Reverse transcription-polymerase chain reaction (RT-PCR) and Real-Time PCR analysis.

Total RNA was extracted from the primary pulp cells with TRIzol® reagent according to the manufacture's instructions (Invitrogen). Total RNA (2 ㎍) was subjected to reverse transcription with 0.5 ㎍ of Oligo d(T) and 1 ㎕ (50 IU) of Superscript III enzyme (Invitrogen) in a 20 ㎕ reaction mixture at 50℃ for 1 h. The resulting mixture was amplified by PCR. One microliter of thereverse transcription product wassubjected to PCR using the following cycling conditions: 94℃, 0.5 min 55℃, 0.5 min 72℃, 1 minfor 32 cycles. The primer sequences used are as follows: 5′-GAC CTG TAC CTG GCC TAC TTT G-3′ and 5′-TTT CCA CCA AAA ATG CAG GCT GG-3′ for *Nfic* 5′-ATG TGG AAA TGG ATA CTG AC-3′ and 5′-CTA TGT TTG GAT CGT CAT GG-3′ for Fgf10 (forward and reverse). As the quantitative control, GAPDH PCR (forward 5′-ACC ACA GTC CAT GCC ATC AC-3′ and reverse 5′-TCC ACC ACC CTG TTG CTG T-3′) was also performed for 20 or 25 cycles using the same cycle profile as used for *Nfic*. The PCR products were electrophoresed on a 1.2% agarose gel, stained with ethidium bromide, and visualized under ultraviolet (UV) light.

For real-time PCR, specific primers for *Nfic*, DSPP, BSP, OC, ALP, collagen type I, DMP1, DMP4, TGFß1, TGFß3 and GAPDH (housekeeping gene for normalization) were synthesized as listed in Table 1. PCR was carried out using

SYBR® Premix Ex TaqTM II (TAKARA, Japan) according to the manufacturer's instructions. Expression quantity was analyzed by ABI PRISM® 7500 (Applied Biosystems, USA). The PCR conditions were 94℃ for 1min followed by 95℃ for 15s and 62℃ for 34s for 40 cycles.

Table 1. Nucleotide sequences of Real Time PCR primer pairs.

gene		primer (5'-3')
Nfic	forward	GACCTGTACCTGGCCTACTTTG
	reverse	CACACCTGACGTGACAAAGCTC
DSPP	forward	ATTCCGGTTCCCCAGTTAGTA
	reverse	CTGTTGCTAGTGGTGCTGTT
BSP	forward	CAGGGAGGCAGTGACTCTTC
	reverse	AGTGTGGAAAGTGTGGCGTT
OC	forward	CTGACAAAGCCTTCATGTCCAA
	reverse	GCGCCGGAGTCTGTTCACTA
ALP	forward	CCAACTCTTTTGTGCCAGAGA
	reverse	GGCTACATTGGTGTTGAGCTTTT
Collagen type I	forward	GCTCCTCTTAGGGGCCACT
	reverse	CCACGTCTCACCATTGGGG

8. MTT assay for cell proliferation.

The proliferation of primary pulp cells was evaluated using the MTT {3-(4,5-Dimethylthiazol-2-yl)-2,5-diphenyltetrazolium bromide, a tetrazole} assay. Primary pulp cells were seeded on 48-well plates at a density of 5 × 103cells/well and cultured. After washing with PBS, 50 ㎕ of MTT (5 mg/ml) was added to each well and incubated for 4 hrs at 37.℃ After removing the MTT solution, the converted dye was dissolved in DMSO and measured by reading the absorbance at a wavelength of 540 ㎚ with a microplate reader (Multiskan EX, Thermo Electron corporation). Triplicate samples were analyzed from two independent experiments.

9. MDPC-23 Cell culture.

MDPC-23 cells (a generous gift from Drs. C.T. Hanks and J. E. Nor, School of Dental Medicine, University of Michigan, MI) were grown and

maintained in Dulbecco's modified Eagle's (DMEM, Gibco BRL) supplemented with 10% fetal bovine serum (FBS, Gibco BRL) and antibiotics (Penicillin-G 100U/ml, Streptomycin 100 ㎍/ml, fungizone 2.5 ㎍/ml, Gibco BRL) at 5% CO2 in a 37℃ incubator.

10. Luciferase assay.

MDPC-23 cells were seeded in 24-well plate at a density of 1 × 105 cells/well and transfected 24 h later using Lipofectamin PLUS reagent (Invitrogen) according to the manufacturer's instruction. For each transfection, 0.4 ㎍ of the luciferase report plasmid and, where indicated 0.4 ㎍ of expression vector, were used. After 24h, cells were incubated 48h with or without 10 ng/ml of TGF-β1 (R&D systems). The cells were lysed for luciferase activity assessment using the luciferase reporter gene assay system (Roche) according to the manufacturer's instructions. Measurements were performed with a luminometer (FLUOStar OPTIMA, BMC Laboratory, Germany).

11. Flow Cytometric analysis for DNA content.

MDPC-23 cells were transiently transfected with the Lipofectamin PULS reagent in Opti-MEM (Invitrogen) containing 2 ㎍ of the control vector (pLKO.1 control), RNAi *Nfic* plasmid (pLKO.1-*Nfic* shRNA). Transfections were performed according to the manufacturer's instruction. The cell cycle was analyzed by flow cytometric quantitation of the DNA contents after propidium iodide (PI) staining. After 72h, the cells were trypsinized, washed in PBS, and fixed in 70% ethanol. For cell cycle analysis, the cells were suspended in PBS containing propidium iodide (10 ㎍/ml) and RNase A (2 ㎍/ml) for 30 min at room temperature, and analyzed by FAC Salibur flow cytometry (BD Bioscience, San Jose, CA).

12. Western blot analysis.

To prepare whole cell extracts, cells were washed 3 times with PBS,

scraped into 1.5ml- tubes and pelleted by centrifugation at 1,000 × g for 5 min at 4℃. After removal ofthe supernatant, the pellet was resuspended in lysis buffer (100 mM Tris, pH 7.4, 350 mM NaCl, 10% glycerol 1% Nonidet P-40, 1 mM EDTA, 1 mM dithiothreitol, 10 ㎍/ml aprotinin, 10 ㎍/ml leupeptin, 10 ㎍/ml pepstatin) and incubated for 15 min on ice. Cell debris was removed by centrifugation at 16,000 × g for 15 min at 4℃. The proteins (30 ㎍) were separated by 10% sodium dodecyl sulfate-polyacrylamide gel electrophoresis (SDS-PAGE) and transferred onto a nitrocellulose membrane (Schleicher & Schuell). The membranes were blocked for 1 h with 5% nonfat dry milk in PBS containing 0.1% Tween-20 (PBS-T), washed with the PBS-T and incubated overnight with primary antibody diluted in PBS-T buffer (1:1000) at 4℃. After washing, the membranes were then incubated with anti-mouse, rabbit or goat-IgG conjugated horseradish peroxidase (Santa Cruz Biotechnology) for 1 h. Labeled protein bands were detected using an enhanced chemiluminescence system (Amersham Biosciences), and bands were measured by densitometric analysis of autoradiograph films.

13. Statistical analysis.

Data was analyzed for statistical significance using a non-parametric Mann-Whitey test.

III. Results

To determine if disruption of the *Nfic* gene causes the phenotypic change of odontoblasts into osteoblasts, I performed light microscopic analysis of morphological changes during ectomesenchymal cell differentiation into odontoblasts in wild type and *Nfic*-deficient mice incisors. A cross-section of an incisor from wild type mice showed the presence of circular dentin and odontoblasts which form a layer lining the periphery of the pulp (Fig. 1A). However, an incisor from *Nfic*-deficient mice contained an open area of the dentin due to the lack of dentin formation. *Nfic*-deficient mice incisors failed to differentiate into normal odontoblasts. These abnormal odontoblasts were round in shape and many of the cells were trapped in osteodentin-like mineralized tissue and therefore resembled osteocytes (Fig. 1B).

If a phenotypicchange from odontoblasts into osteoblasts occurs as a result of loss of *Nfic*, the abnormal odontoblast-like cells are expected to lose or have a decreased ability to express dentin sialophosphoprotein (DSPP). To test this hypothesis, I performed immunohistochemical analysis of DSPP expression in *Nfic*-deficient mice incisors. Wild type odontoblasts demonstrate strong DSPP protein expression (Fig. 1C), while abnormal odontoblasts exhibited a decreased level of DSPP protein expression (Fig. 1D).

To determine whether the mineralized tissue formed by abnormal odontoblasts in *Nfic*-deficient mice incisors contains bone sialoprotein (BSP), cross-sections of the incisors from wild type and *Nfic*-deficient mice were prepared to compare the immunohistochemical localization of BSP. Inwild type incisors, BSP expression was restricted to a thin layer of cementum that covers the dentin but is absent within the dentin (Fig. 1E). In contrast, strong BSP expression was observed not only in the newly formed mineralized tissue formed by aberrant odontoblasts within *Nfic*-deficient mice incisors, but also in the areas where abnormal odontoblasts were located (Fig. 1F).

Dentin and bone matrix gene expression was analyzed by real-time PCR in primary pulp cells from wild type and *Nfic*-deficient incisors. DSPP, osteocalcin, ALP, type I collagen, DMP1, and DMP4 expression was decreased in the *Nfic*-deficient primary pulp cells compared to wild type cells (Fig. 2A). However, BSP expression was increased in *Nfic*-deficient primary pulp cells (Fig. 2A). Additionally, TGF-β1 and TGF-β3 were also up-regulated in the *Nfic*-deficient primary pulp cells (Fig. 2B).

TGF-β1 is known to down-regulate DSPP expression (25), whereas it up-regulate BSP expression (26). Therefore, to determine whether disruption of *Nfic* gene down-regulates DSPP and up-regulates BSP expression due to the up-regulation of TGF-β1, I measured DSPP and BSP promoter activity in MDPC-23 cells. As expected, DSPP promoter activity decreased upon TGF-β1 treatment,as well as when Smad2 and Smad3 were over-expressed compared to untreated cells, but siRNA inactivation of *Nfic* did not lead to a decrease in DSPP promoter activity (Fig. 2C). In contrast, over-expression of *Nfic* led to a decrease in DSPP promoter activity (Fig. 2C). On the other hand, BSP promoter activity increased following siRNA inactivation of *Nfic*, TGF-β1 treatment, or over-expression of Smad2 compared to untreated cells, whereas over-expression of *Nfic* and Smad3 led to a decrease in BSP promoter activity (Fig. 2D).

To understand the mechanism by which the loss of *Nfic* causes short root formation, the expression of p-Smad2/3 was investigated using immunohistochemistry. Although p-Smad2/3 was barely detected in cells extracted from the incisors from wild type mice (Figs. 3A, C), it was strongly detected in incisors from *Nfic*-deficient mice (Figs. 3B, D). Similar results were also found in the molars from normal and *Nfic*-deficient mice (data not shown). To confirm these findings, the expression of the TGFβ-RI and p-Smad2/3 was examined in primary pulp cell cultures from normal as well as *Nfic*-deficient mice. Western blot analysis revealed a dramatic increase in the expression of TGFβ-RI and p-Smad2/3 in the *Nfic*-deficient primary pulp cells compared to that of wild type (Figs. 3E, F).

To determine if the formation of short roots in *Nfic*-deficient mice is the result of decreased cell proliferation of cervical loop and EM cells, cell proliferation was assessed and compared between wild type and *Nfic*-deficient mice using BrdU labeling. The number of BrdU-labeled cervical loop and EM cells in the incisors of wild type mice (Figs. 4A, C) was much higher than that in *Nfic*-deficient mice (Figs. 4B, D), and was reduced by 2.5 ~ 5 fold in the *Nfic*-deficient mice (Fig. 4E).

Previously, it was reported that fibroblast growth factor 10 (FGF10) is important for the maintenance of the stem cell niche of the dental epithelium and for the continuous growth of the mouse incisor (27). I therefore examined expression of FGF10 by RT-PCR in primary pulp cells. My data show that FGF10 was significantly decreased in *Nfic*-deficient primary pulp cells compared to wild type (Figs. 4F, G).

The influence of *Nfic* on cell proliferation was further investigated in vitro using the MTT assay. The proliferation rates of *Nfic*-deficient primary pulp cells were found to be decreased by 13 % compared to their wild type counterparts when cells were cultured for up to 7 days (Fig. 5A).

The influence of *Nfic* on cell cycle control was analyzed by examining the cellular DNA content using a flow cytometer following propidium iodide (PI) staining of MDPC-23 cells. The population of S phase cells in *Nfic* siRNA-inactivated MDPC-23 cells was increased by 13.41%, compared to control cells, while the populations in G1 and G2/M phases decreased, indicating S phase arrest (Fig. 5B).

Cell cycle related proteins and cyclin dependant kinase inhibitors are known to regulate cell proliferation (28). To investigate whether any of these proteins are involved in the cell growth arrest caused by the loss of *Nfic*, the expression of p21, p16, cyclin D1, and cyclin B1 were examined in *Nfic*-deficient primary pulp cells by western blot analysis. *Nfic*-deficient primary pulp cells exhibited an increase in p21 as well as p16 expression, and a decrease in cyclin D1 as well as cyclin B1 expression compared with wild type cells (Figs. 5C, D).

To examine if short root formation in *Nfic*-deficient mice is due to an increase in apoptosis of pulp cells and odontoblasts during root development, TUNEL-POD staining in incisor histological sections from P17 wild type and *Nfic*-deficient mice was performed. Compared to wild type mice (Figs. 6A, C), *Nfic*-deficient mice demonstrated an increase in apoptotic pulp cells, preodontoblastic cells in the sub-odontoblastic layer, and aberrant odontoblasts trapped in abnormal dentin (Figs. 6B, D).

The expression of caspase 3 and 8, the central players of apoptosis, in *Nfic*-deficient primary pulp cells was examined by western blot analysis. Both the expression and level of cleavage of caspase-8,known as the general initiator caspase, were higher in *Nfic*-deficient primary pulp cells compared to that of wild type. The level of caspase-8 cleavage was also higher in *Nfic*-deficient primary pulp cells (Figs. 7A, B). Active caspase-8 can cleave and activate procaspase-3, which leads to apoptosis. The level of caspase-3 expression was also higher in *Nfic*-deficient primary pulp cells, and cleaved caspase-3 was detected in *Nfic*-deficient primary pulp cells (Figs. 7C, D).

I next examined the expression of Bid, a mitochondria-related apoptosis effector that is cleaved by caspase-8 (29). The level of Bid expression was equivalent between normal and *Nfic*-deficient primary pulp cells, and no Bid cleavage was detected (Figs. 7E, F). The anti-apoptotic Bcl-2 family, including Bcl-2 and Bcl-XL, was also examined by RT-PCR and western blot analysis. The level of Bcl-XL remained unchanged, but the level of Bcl-2 was higher in *Nfic*-deficient primary pulp cells than wild type primary pulp cells (data not shown). xIAP and cIAP1/2 are direct caspase inhibitors and are known to bind to and inhibit activated caspase-3, -7, and procaspase-9 (29). Western blot analysis showed that the expression level of cIAP1/2 was lower in *Nfic*-deficient primary pulp cells than controls (Figs. 7E, F).

Ⅳ. *Discussion*

The author previously reported that *Nfic*-deficient mice develop short roots with aberrant odontoblasts that exhibit unique morphological features (24). Unlike normal odontoblasts, they display a rounded shape and lack the cellular polarization and organization normaly seen in the odontoblasts layer. Further, aberrant odontoblasts become dissociated and trapped in an osteodentin-like mineralized tissue. Interestingly, when TGF-β1 is overexpressed predominantly in odontoblasts using a transgenic construct consisting of a dentin sialophosphoprotein regulatory sequence and TGF-β1 cDNA, the transgenic mice revealed the same phenotypic changes of odontoblasts as seen in *Nfic*-deficient mice (20). These transgenic animal studies strongly suggest a functional relationship between *Nfic* and Smads in odontoblast development.

In the present study, *Nfic*-deficient mice demonstrated a higher expression level of TGFβ-RI and p-Smad2/3 than wild type mice. Furthermore, *Nfic*-deficient mice showed a decrease in DSPP expression, but an increase in BSP expression. Although siRNA inactivation of *Nfic* had no effect on DSPP promoter activity, BSP promoter activity was increased. In addition, overexpression of Smad2 led to an up-regulation of BSP, while over-expression of Smad3 led to the down-regulation of BSP in MDPC-23 cells. It has previously been reported that Smad2 and Smad3 may play distinct roles in mediating TGF-β signaling in MDPC-23 cells (23). This led us to speculate that the increased TGF-β signaling observed in *Nfic*-deficient mice may be a direct result of the inactivation of the *Nfic* and is responsible for the aberrant odontoblasts and short root formation in *Nfic*-deficient mice. This hypothesis is supported by a recent study that compared the DNA binding domains of Smads and NFI transcriptional factors (30). According to a sensitive PSI-Blast database research, these transcriptional factors share significant similarities in their DNA binding domains and may belong to a new superfamily of genes (31). The

possible functional relationship between these two transcriptional factors in odontoblastsdifferentiation and functions during root formation is currently under investigation.

In the apical region of developing roots, both cervical loop and EM cells actively proliferate and thus their well-coordinated cell proliferation plays a crucial role in normal root formation (4). In particular, the EM cells adjacent to the cervical loop differentiate into odontoblasts that are responsible for root dentin formation. I found that *Nfic*-deficient mice had less BrdU-positive cervical loop and EM cells in the apical end of mandibular incisors than wild type mice. Previous studies showed that FGF10 plays a key role in the developing tooth by stimulating proliferation and differentiation of cervical loop stem cells. It was reported that mouse incisors EM cells express FGF10, while its receptor, FGFR2b, is expressed throughout the cervical loop epithelium. In addition, the cervical loop of FGF-deficient mice showed a decreased in cell proliferation (27).

In the present study, *Nfic*-deficient primary pulp cells were shown to express a decreased level of FGF10 compared to wild type cells. Recently, it has been reported that TGF-β1 down-regulates FGF10 in the lung (32) and the prostate (33). Likewise, *Nfic*-deficient primary pulp cells showed a decreased in proliferation activity in vitro when compared to control cells. p21 has been shown to plays a key role in cell growth arrest at the G1/S checkpoint by inhibiting the activity of cyclin E/Cdk2, cyclin D1/Cdk4/6, cyclin A/Cdk2, and to a lesser extent, cyclin B/Cdc2 (28). Furthermore, p16 inhibits cyclin D/Cdk4/6 thereby preventing the inactivation of pRB (34). Interestingly, *Nfic* gene inactivation led to an increase in the expression of cell cycle inhibitors such as p21 and p16 which is in agreement with a recent finding that NFI is a key repressor of p21 transcription (35). Further, TGF-β has been shown to inhibit cell cycle progression partially through the up-regulation of expression of p21, p15 and p27 cell cycle inhibitors (36). Smads also play an important role in the regulation of p21 in HaCaT cells (37). These findings suggest that the loss of

the *Nfic* gene may decrease the proliferation of cervical loop and EM cells through an increase in p21 expression and decrease in FGF10 expression in EM cells, and may contribute in part to short root formation.

Apoptosis is an essential physiological process that plays a critical role in development and tissue homeostasis (38). During tooth development, apoptosis occurs at all stages: early tooth morphogenesis (39), amelogenesis (40), dentinogenesis (41), and tooth eruption (42). The specific temporospatial appearance of apoptotic cells during tooth development suggests its important role in odontogenesis (43). In the present study, the appearance of apoptotic cells was evident in the sub-odontoblastic region of developing roots from *Nfic*-deficient mice, and more prominent in the area where aberrant odontoblasts trapped in abnormal dentin are located. However, little is known about the causes and signaling pathways responsible for odontoblast apoptosis. Previous studies showed that TGF-β1 induces apoptosis in MDPC-23 cells via in Smad-dependent pathway (23). Our findings suggest that inactivation of the *Nfic* leads to the up-regulation of TGF-β1 expression which thereby induces the expression of Smad 2/3 in odontogenic cells. I therefore speculate that odontogenic cells in *Nfic*-deficient mice may undergo apoptosis via Smad dependant pathways resulting in short root formation.

Inhibitors of apoptosis (IAPs cIAP1/2 and xIAP) are direct caspase inhibitors which bind to and inhibit active caspase-3 and -7, the key effectors of apoptosis (29). Recently, activated caspase-3 was detected in the primary enamel knot of the filed vole (44), but little is known about the activation of other caspases such as caspase-8 and -9. In the present study, the expression of caspase-3 and -8 was found to be increased, while c-IAP1/2 was decreased in *Nfic*-deficient primary pulp cells. It is known that the mitochondrial apoptotic pathway is initiated through caspase-8-mediated Bid cleavage (45), but I could not detect any cleaved form of Bid. However, even though the expression of Bcl-XL, an anti-apoptotic member of the Bcl-2 family, remained unchanged, the expression of Bcl-2 was increased in *Nfic*-deficient primary pulp cells (data not

shown). These findings suggest that procaspase-3, which is cleaved directly by activated caspase-8, but not by the mitochondrial apoptotic pathway, may also be involved in apoptosis of *Nfic*-deficient primary pulp cells.

In the present study, wild type mice exhibited normal circular dentin but *Nfic*-deficient mice contained abnormal dentin, osteodentin. In *Nfic*-deficient mice, the labial side of an incisor exhibited osteodentin, while the lingual side showed an open area of the dentin due to the lack of dentin formation. Dentin is covered by enamel and ameloblast in the labial side of an incisor, whereas it is not covered in the lingual side. Interestingly, ameloblast (ALC)-conditioned media facilitated the differentiation and mineralization of MDPC-23 cells compared to their control counterparts (data not shown). ALC conditioned media also affected the expression of *Nfic* during odontoblast differentiation (data not shown). Therefore, these results suggest a link between ameloblasts and odontoblasts during tooth development, through NF1-C. This speculation requires further investigation.

In conclusion, *Nfic* appears to play an important role in the proliferation of odontogenic cells, their differentiation into odontoblasts, and odontoblasts survival during root formation. Therefore, inactivation of the *Nfic* gene may result in short root formation.

References

1. Smith, A. J., and Lesot, H. (2001) Crit. Rev. Oral Biol. Med. 12(5), 425-437

2. Sharpe, P. T. (2001) Adv. Dent. Res. 15, 4-7

3. Zeichner-David, M., Oishi, K., Su, Z., Zakartchenko, V., Chen, L. S., Arzate, H., and Bringas, P. Jr., (2003) Dev. Dyn. 228(4), 651-663

4. Kaneko, H., Hashimoto, S., Enokiya, Y., Ogiuchi, H., and Shimono, M. (1999) Cell. Tissue. Res. 298(1), 95-103

5. Luan, X., Ito, Y., and Diekwisch, T. G. (2006) Dev. Dyn. 235(5), 1167-1180

6. Nagata, K., Guggenheimer, R., Enomoto, T., Lichy, J., and Hurwitz, J. (1982) Proc. Natl. Acad. Sci. U.S.A. 79(21), 6438-6442

7. Gronostajski, R. M. (2000) Gene 249(1-2), 31-45

8. Chaudhry, A. Z., Lyons, G. E., and Gronostajski, R. M. (1997) Dev. Dyn. 208(3), 313-325

9. Shu, T., Butz, K. G., Plachez, C., Gronostajski, R. M., and Richards, L. J. (2003) J. Neurosci. 23(1), 203-212

10. Steele-Perkins, G., Plachez, C., Butz, K. G., Yang, G., Bachurski, C. J., Kinsman, S. L., Litwack, E. D., Richards, L. J., and Gronostajski, R. M. (2005) Mol. Cell. Biol. 25(2), 685-698

11. Gründer, A., Ebel, T. T., Mallo, M., Schwarzkopf, G., Shimizu, T., Sippel, A.

E., and Schrewe, H. (2002) Mech. Dev. 112(1-2), 69-77

12. Driller, K., Pagenstecher, A., Uhl, M., Omran, H., Berlis, A., Gründer, A., and Sippel, A. E. (2007) Mol. Cell. Biol. 27(10), 3855-3867

13. Steele-Perkins, G., Butz, K. G., Lyons, G. E., Zeichner-David, M., Kim, H. J., Cho, M. I., and Gronostajski, R. M. (2003) Mol. Cell. Biol. 23(3), 1075-1084

14. Lee, K. Y., and Bae, S. C. (2002) J. Biochem. Mol. Biol. 35(1), 47-53

15. Siegel, P. M., and Massagué, J. (2003) Nat. Rev. Cancer 3(11), 807-821

16. Sanchez-Capelo, A. (2005) Cytokine Growth Factor Rev. 16(1), 15-34

17. Schuster, N., and Krieglstein, K. (2002) Cell Tissue Res. 307(1), 1-14

18. Miyazono, K., Kusanagi, K., and Inoue, H. (2001) J. Cell. Physiol. 187(3), 265-276

19. Smith, A. J., Matthews, J. B., and Hall, R. C. (1998) Eur. J. Oral Sci. 106(suppl1), 179-184

20. Thyagarajan, T., Sreenath, T., Cho, A., Wright, J. T., and Kulkarni, A. B. (2001) J. Biol. Chem. 276(14), 11016-11020

21. Hanks, C. T., Sun, Z. L., Fang, D. N., Edwards, C. A., Wataha, J. C., Ritchie, H. H., and Butler, W. T. (1998) Connect. Tissue Res. 37(3-4), 233-249

22. Sun, Z. L., Fang, D. N., Wu, X. Y., Ritchie, H. H., Begue-Kirn, C., Wataha, J. C., Hanks, C. T., and Butler, W. T. (1998) Connect. Tissue Res. 37(3-4),

251-261

23. He, W. X., Niu, Z. Y., Zhao, S. L., and Smith, A. J. (2005) Arch. Oral Biol. 50(11), 929-936

24. Park, J. C., Herr, Y., Kim, H. J., Gronostajski, R. M., and Cho, M. I. (2007) J. Periodontol. 78(9), 1795-1802

25. He, W. X., Niu, Z. Y., Zhao, S. L., Jin, W. L., Gao, J., and Smith, A. J. (2004) Arch. Oral Biol. 49(11), 911-918

26. Ogata, Y., Niisato, N., Furuyama, S., Cheifetz, S., Kim, R. H., Sugiya, H., and Sodek, J. (1997) J. Cell. Biochem. 65(4), 501-512.

27. Harada, H., Toyono, T., Toyoshima, K., Yamasaki, M., Itoh, N., Kato, S., Sekine, K., and Ohuchi, H. (2002) Development 129(6), 1533-1541.

28. Shackelford, R. E., Kaufmann, W. K., and Paules, R. S. (2000) Free Radical Biol. Med. 28(9), 1387-1404

29. Philchenkov, A. A. (2003) Biochemistry (Moscow) 68(4), 365-376

30. Stefancsik, R., and Sarkar, S. (2003) DNA Sequence 14(4), 233-239

31. Iozzo, R. V., Pillarisetti, J., Sharma, B., Murdoch, A. D., Danielson, K. G., Uitto, J., and Mauviel, A. (1997) J. Biol. Chem. 272(8), 5219-5228

32. Chen, F., Desai, T. J., Qian, J., Niederreither, K., Lü, J., and Cardoso, W. V. (2007) Development 134(16), 2969-2979.

33. Tomlinson, D. C., Grindley, J. C., and Thomson, A. A. (2004) Endocrinology.

145(4), 1988-1995.

34. Cox, L. S. (1997) J. Pathol. 183(2), 134-140

35. Ouellet, S., Vigneault, F., Lessard, M., Leclerc, S., Drouin, R., and Guérin, S. L. (2006) Nucleic Acids Res. 34(22), 6472-6487

36. Gong, J., Ammanamanchi, S., Ko, T. C., and Brattain, M. G. (2003) Cancer Res. 63(12), 3340-3346

37. Pardali, K., Kurisaki, A., Morén, A., ten Dijke, P., Kardassis, D., and Moustakas, A. (2000) J. Biol. Chem. 275(38), 29244-29256

38. Schultz, D. R., and Harrington, W. J. Jr. (2003) Semin. Arthritis Rheum. 32(6), 345-369

39. Shigemura, N., Kiyoshima, T., Kobayashi, I., Matsuo, H., Akamine, A., and Sakai, H. (1999) Histochem. J. 31(6), 367-377

40. Bronckers, A. L., Goei, S. W., Dumont, E., Lyaruu, D. M., Wöltgens, J. H., van Heerde, W. L., Reutelingsperger, C. P., and van den Eijnde, S. M. (2000) Histochem. Cell Biol. 113(4), 293-301

41. Vermelin, L., Lécolle, S., Septier, D., Lasfargues, J. J., and Goldberg, M. (1996) Eur. J. Oral. Sci. 104(5-6), 547-553

42. Ten Cate, A. R., and Anderson, R. D. (1986) J. Dent. Res. 65(8), 1087-1093

43. Matalova, E., Tucker, A. S., and Sharpe, P. T. (2004) J. Dent. Res. 83(1), 11-16

44. Shigemura, N., Kiyoshima, T., Sakai, T., Matsuo, K., Momoi, T., Yamaza, H., Kobayashi, I., Wada, H., Akamine, A., and Sakai, H. (2001) Histochem J. 33(5), 253-258

45. Zimmermann, K. C., Bonzon, C., and Green, D. R. (2001) Pharmacol. Ther. 92(1), 57-70

Figure legends

Fig. 1. Light micrographs showing cross section of P10 incisors from wild type and *Nfic*-deficient mice. (A) A wild type incisor showing a circular ring of dentin and odontoblasts that line the inner surface of dentin. (B) *Nfic*-deficient incisor showing an open area (*) due to the lack of dentin formation caused by abnormal odontoblasts. Note thick osteodentin-like mineralized tissue that contains numerous trapped cells (arrowheads). (H&E stained, A and B). Immunohistochemical localization of DSPP (C and D) and BSP (E and F)in wild type and *Nfic*-deficient incisor. (C) DSPP is strongly expressed in wild type odontoblasts but not in pulp. (D) DSPP is weakly detected in abnormal odontoblasts that are trapped in osteodentin-like mineralized tissue as well as lining the inner osteodentin-like mineralized tissue showing little expression (arrowheads). (E) BSP is localized primarily in the cementum (arrowhead) along the dentin surface and bone in wild type incisors. (F) BSP is observed in cementum along the dentin surface, newly formed osteodentin-like mineralized tissue (*), and areas occupied by abnormal odontoblasts (arrow) in *Nfic*-deficient incisors. Am, ameloblasts; O, odontoblasts; OD, osteodentin-like mineralized tissue P, pulp B, bone. (A, C and E Scale bar = 100 ㎛ B Scale bar = 50 ㎛. D, F Scale bar = 20 ㎛.)

Fig. 2. Real time PCR and promoter activity analysis.Expression of dentin, bone matrix gene (A), TGF-β1and TGF-β3 (B) was analyzed by real-time PCR in primary pulp cells. DSPP (C) and BSP (D) promoter activity measured in MDPC-23 cells. Cells were co-transfected with pGL3LUC-791~+54 under control of the DSPP promoter, or pGL3LUC-2744~+60 under control of the BSP promoter, as indicated in Material & Methods, or the control empty vector pGL3-basic. After 24h of transfection, cells were incubated for 48 h with or without 10 ng/ml of TGF-β1, and luciferase activity was analyzed. The results

represent data from three separated transfections, with standard errors. * denotes values significantly different from control (* P<0.01).

Fig. 3. TGFβ-RI and p-Smad2/3 were expressed strongly in the incisors of *Nfic*-deficient mice. Expression of p-Smad2/3 in P17 incisors from the wild type and *Nfic*-deficient mice was analyzed by immunohistochemistry. The number of p-Smad2/3 immunoreactive cells is greater in the sub-odontoblasts and pulp of *Nfic*-deficient mice (B, D) than in the wild type mice (A, C). (E) Evaluation of TGF-βRI, p-Smad2/3 and *Nfic* protein expression. Whole cell lysateswere purified from primary pulp cells and separated by SDS-PAGE. Western blot analysis was carried out using anti-*Nfic*, anti-TGFβ-RI, and anti-p-Smad2/3 antibodies, and normalized to GAPDH as an internal control. (F) Bands were measured by densitometric analysis of autoradiograph films. Panels C and D are higher magnifications of boxed panels A and B, respectively. Sagittal section. Am, ameloblasts; P, pulp. (A, B Scale bar = 50 ㎛ C, D Scale bar = 20 ㎛.)

Fig. 4. Proliferation activity is lower in *Nfic*-deficient mice. Proliferation activity was analyzed by measuring BrdU incorporation in the P10 incisors of normal (A, C) and *Nfic*-deficient mice (B, D). BrdU- labeled cells were detected in the cervical loop and EM cells of wild type mice. The proliferation activity was lower in *Nfic*-deficient mice than in wild type mice. (E) Quantification of BrdU-labeled cells in the cervical loop and EM cells in the incisors of normal and *Nfic*-deficient mice. The total number of BrdU-positive cells was lower in the pulp and cervical loop and EM cells in *Nfic*-deficient mice. (F) Evaluation of FGF10 mRNA expression in primary pulp cells. Total RNA was isolated from the primary pulp cells, and the expression of FGF10 mRNA levels was analyzed by RT-PCR. (G) Bands were measured by densitometric analysis. Data is presented as the mean ± S.D. Significant differences in the mitotic indices between the three groups (with error bars) was calculated using a

non-parametric Mann-Whitney test (* $p<0.05$). Panels C and D are higher magnifications of boxed panels A and B, respectively. Sagittal sections. Am, ameloblasts; Od, odontoblasts; P, pulp or EM, ectomesenchyme. (A, B Scale bar = 50 ㎛ C, D Scale bar = 20 ㎛.)

Fig. 5. Loss of *Nfic* prevents cell cycle progression due to p21 over-expression in primary pulp cells. (A) Cell proliferation assay. Primary pulp cells were seeded on 48-well plates at a density of 5 × 103 cells/well and cultured. Cell proliferation was evaluated by the MTT assay at 1-, 3-, 5-, and 7-days. The data is presented as the mean ± S.D. of three independent experiments (* $p<0.05$). (B) Flow cytometric analysis of cell growth arrest in MDPC-23 cells. MDPC-23 cells were transiently transfected with 2 ㎍of the control vector (pLKO.1 control) and RNAi *Nfic* plasmid (pLKO.1-*Nfic* shRNA) as described in Material and Methods. After 72 h, the cells were harvested, fixed with 70% ethanol, and stained with propidium iodide (PI). DNA content was determined by flow cytometery. (C) Evaluation of p21, p16, cyclin D1, and cyclin B1 protein expression. Whole cell lysates were obtained from primary pulp cells and separated by SDS-PAGE. Western blot analysis was carried out using anti-p21 and anti-cyclin B1 antibodies. (D) Bands were measured by densitometric analysis of autoradiograph films.

Fig. 6. Loss of the *Nfic* increases apoptotic activity in primary pulp cells. TUNEL-POD staining of P17incisors from the wild type (A, C) and *Nfic*-deficient mice (B, D). More TUNEL-positive cells were detected in the odontoblasts (Od) of *Nfic*-deficient mice compared to wild type mice. Apoptotic cells were detected in a sub-odontoblastic location (arrow), and were more numerous in the aberrant odontoblasts trapped in abnormal dentin (arrowheads) of *Nfic*-deficient mice. Panels C and D show higher magnifications of boxed panels A and B, respectively. Cross section. Am, ameloblasts; Od, odontoblasts; P, pulp. (A Scale bar = 100 ㎛ B Scale bar = 50 ㎛ C, D Scale bar = 20 ㎛.)

Fig. 7. Loss of *Nfic* inducesapoptosis through the activation of caspases in primary pulp cells. Evaluation of caspase-8 (A, B)and caspase-3 proteins (C, D). Evaluation of Bid and cIAP1/2 proteins (E, F). Whole cell lysates were obtained from primary pulp cells and separated by SDS-PAGE. Western blot analysis was carried out using anti-caspase-8, anti-caspase-3, anti-Bid, and anti-cIAP1/2 antibodies. Bands were measured by densitometric analysis of autoradiograph films (B, D, and F).

Figures

Figure 1

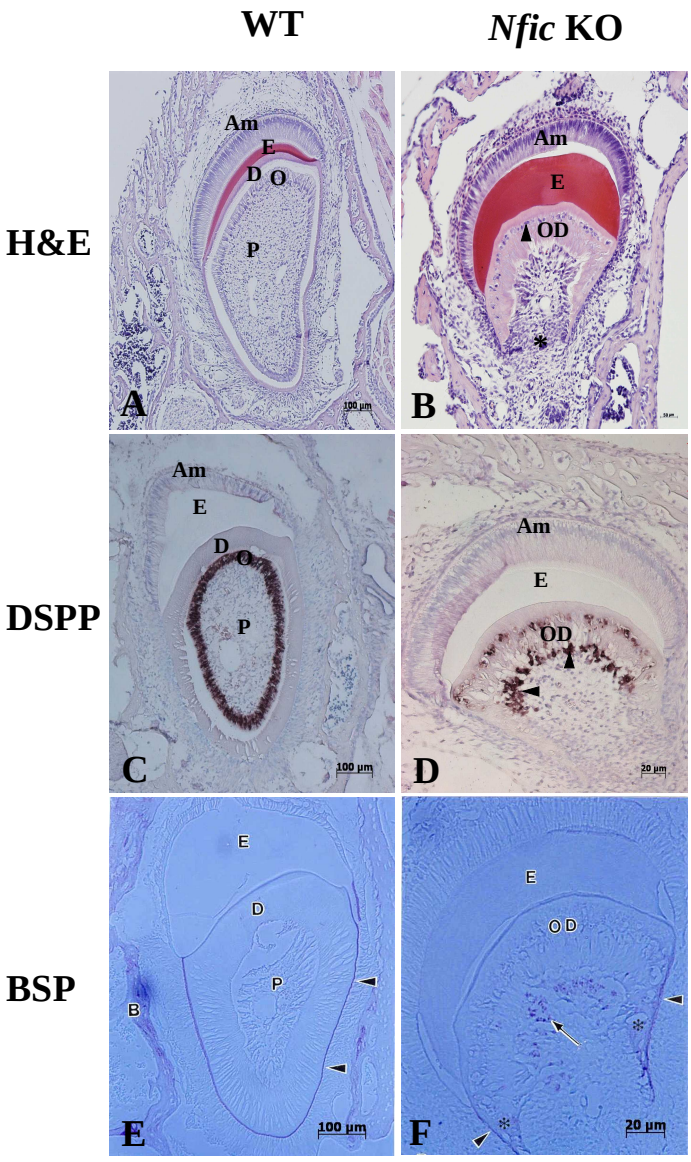

Figure 2

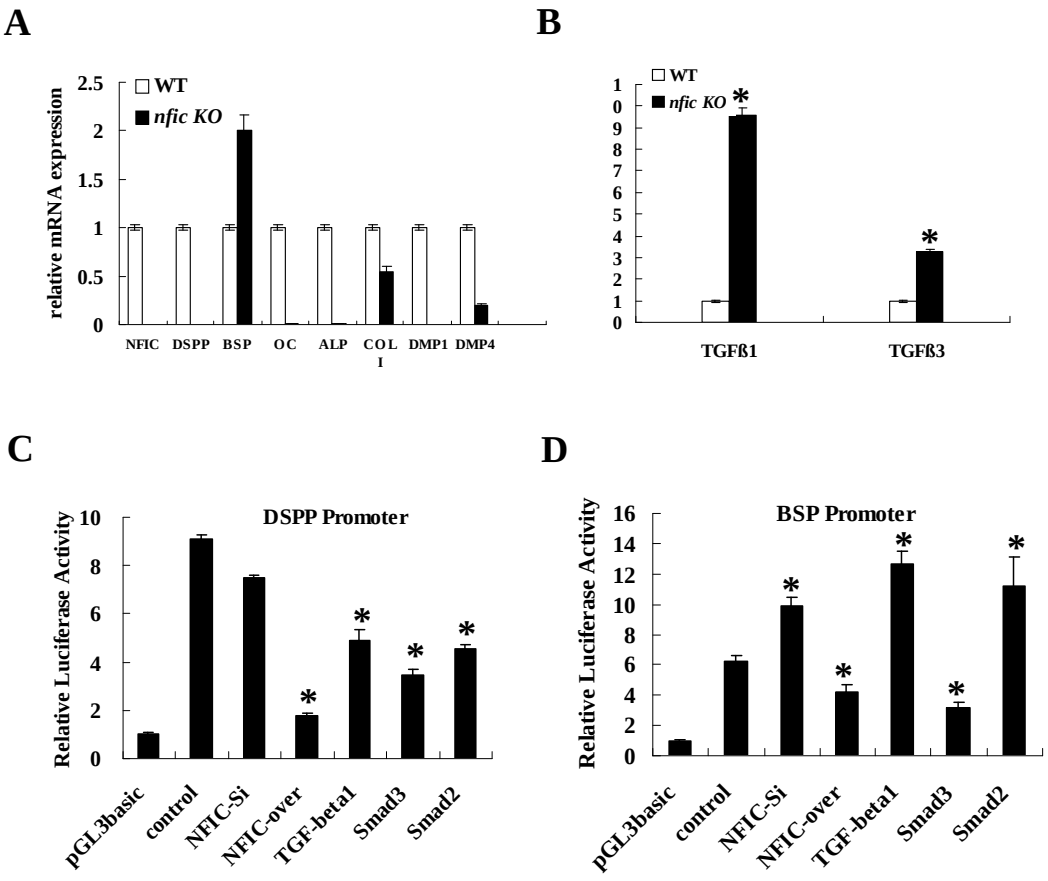
A
WT
nfic KO
relative mRNA expression
2.5
2
1.5
1
0.5
0
NFIC
DSPP
BSP
OC
ALP
COL I
DMP1
DMP4
B
WT
nfic KO
*
*
TGFß1
TGFß3
C
DSPP Promoter
Relative Luciferase Activity
pGL3basic
control
NFIC-Si
NFIC-over
TGF-beta1
Smad3
Smad2
D
BSP Promoter
Relative Luciferase Activity
pGL3basic
control
NFIC-Si
NFIC-over
TGF-beta1
Smad3
Smad2

Figure 3

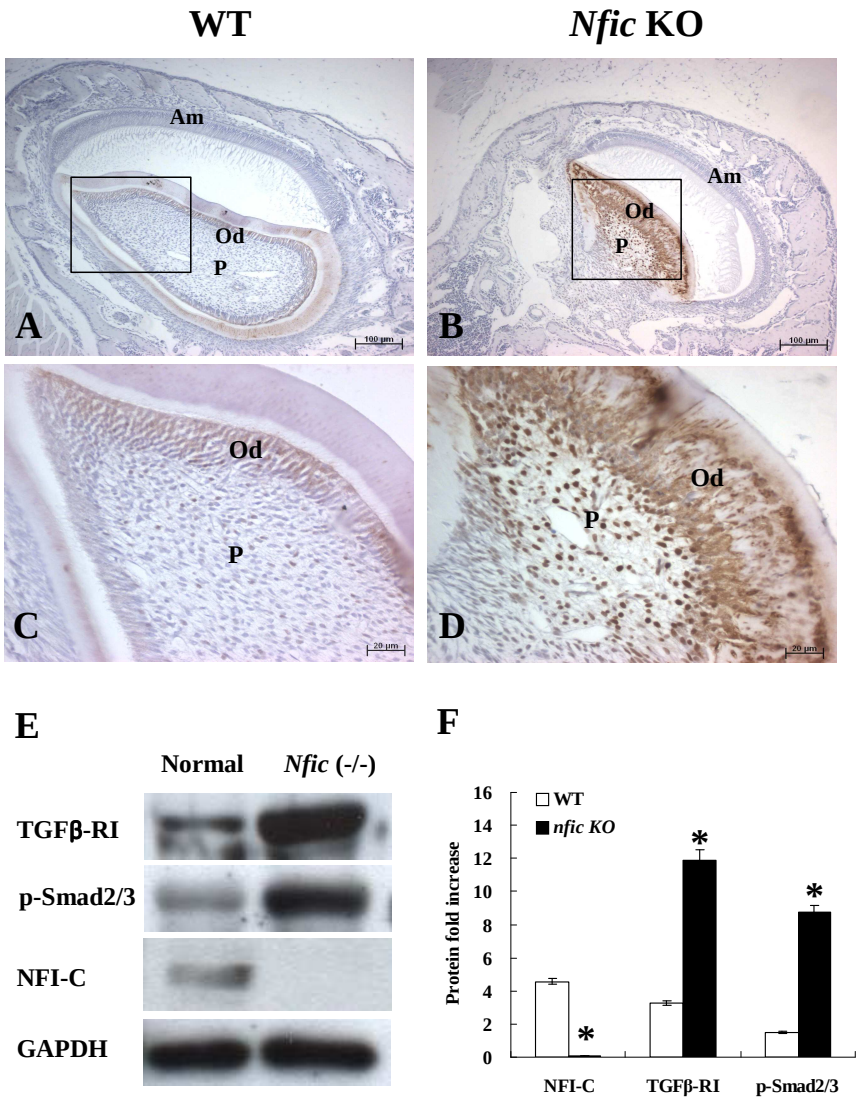
WT
Nfic KO
Am
Od
P
A
B
C
D
E
Normal
Nfic (-/-)
TGFβ-RI
p-Smad2/3
NFI-C
GAPDH
F
WT
nfic KO
Protein fold increase
16
14
12
10
8
6
4
2
0
NFI-C
TGFβ-RI
p-Smad2/3

Figure 4

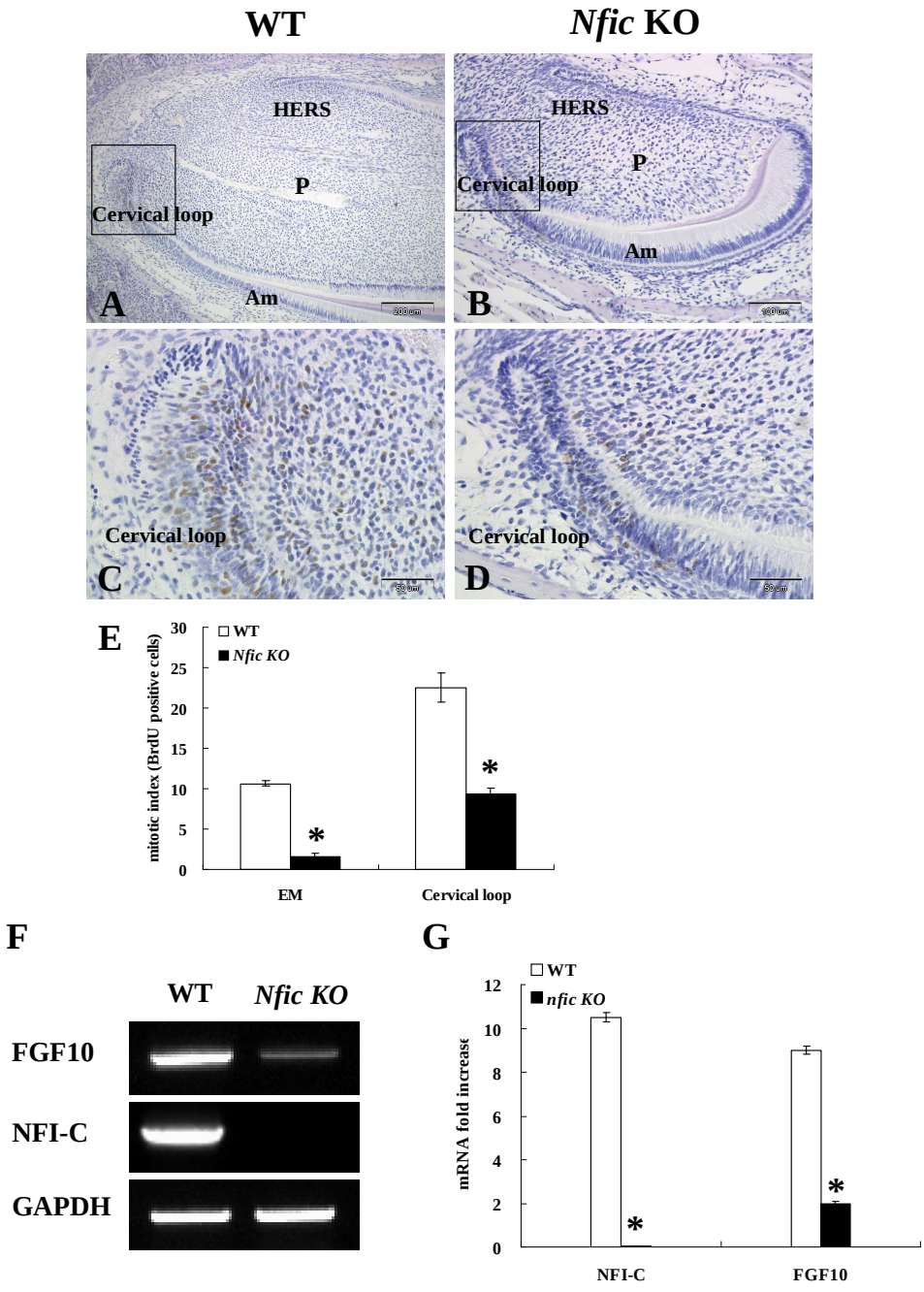
WT
Nfic KO
HERS
P
Cervical loop
Am
A
B
C
D
E
WT
Nfic KO
mitotic index (BrdU positive cells)
EM
Cervical loop
F
WT
Nfic KO
FGF10
NFI-C
GAPDH
G
WT
nfic KO
mRNA fold increase
NFI-C
FGF10

Figure 5

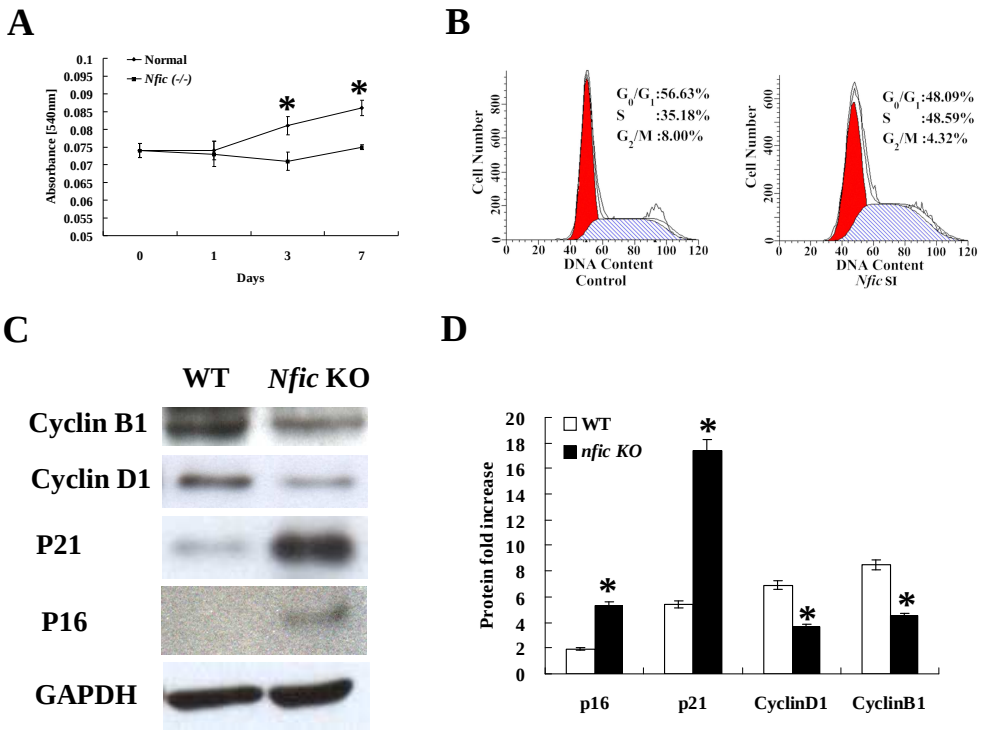
A
Normal
Nfic (-/-)
Absorbance [540nm]
Days
B
Cell Number
DNA Content
Control
G0/G1:56.63%
S :35.18%
G2/M :8.00%
Nfic SI
G0/G1:48.09%
S :48.59%
G2/M :4.32%
C
WT
Nfic KO
Cyclin B1
Cyclin D1
P21
P16
GAPDH
D
WT
nfic KO
Protein fold increase
p16
p21
CyclinD1
CyclinB1

Figure 6

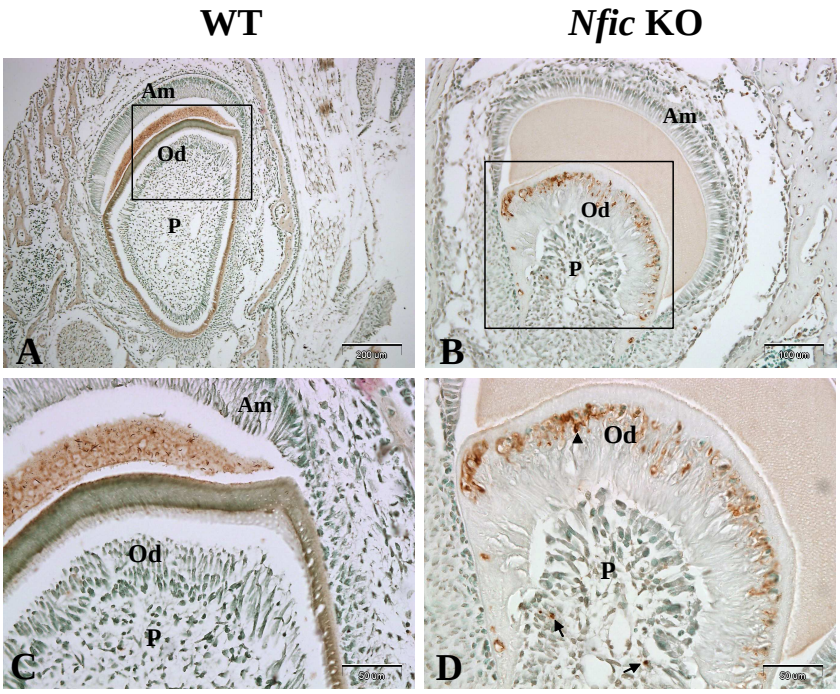

Figure 7

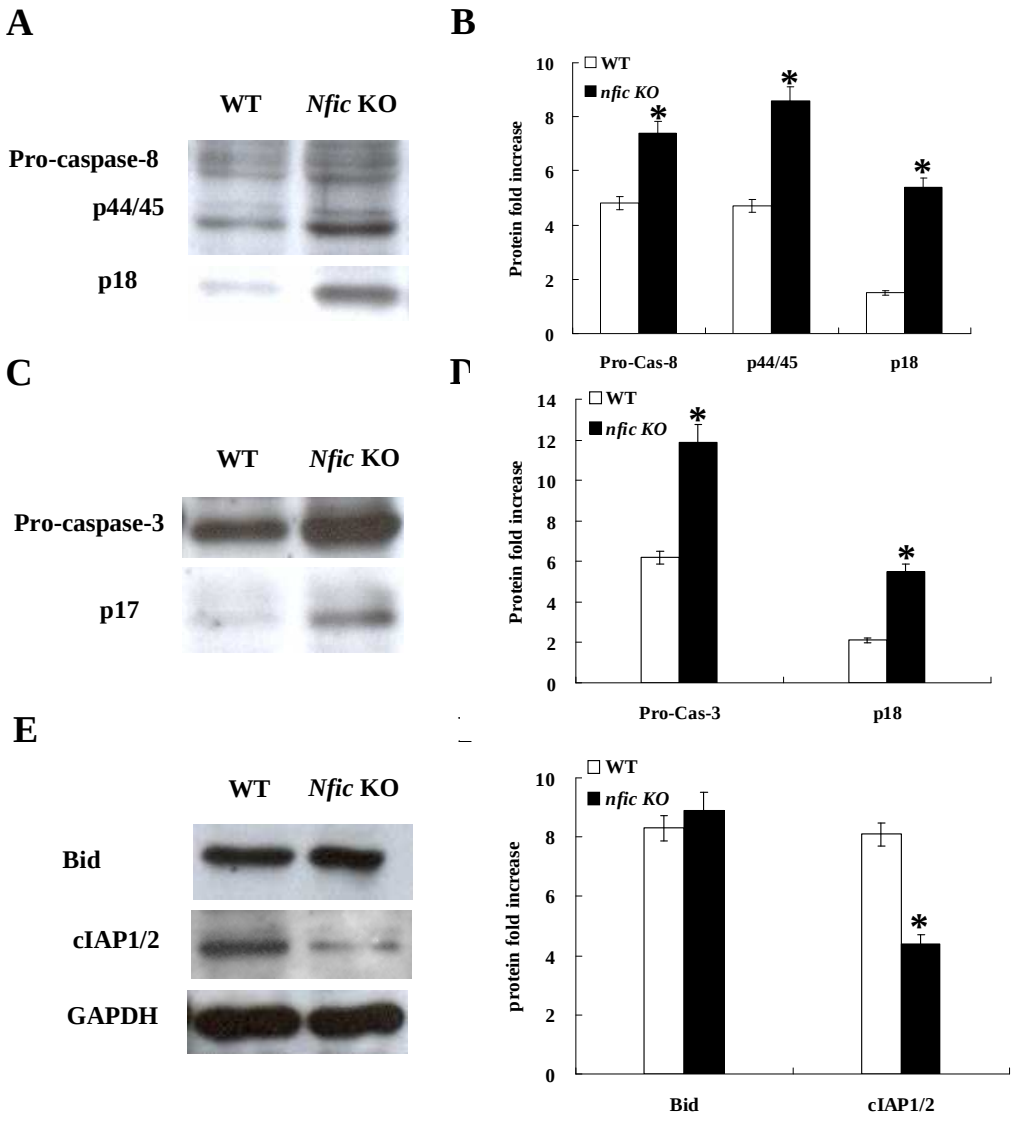
A
WT
Nfic KO
Pro-caspase-8
p44/45
p18
B
WT
nfic KO
Protein fold increase
Pro-Cas-8
p44/45
p18
C
WT
Nfic KO
Pro-caspase-3
p17
Г
WT
nfic KO
Protein fold increase
Pro-Cas-3
p18
E
WT
Nfic KO
Bid
cIAP1/2
GAPDH
WT
nfic KO
protein fold increase
Bid
cIAP1/2

Abstract in Korean

Nfic 유전자 결손이 상아모세포 분화와 상아질 형성에 미치는 영향

김 지 웅

조선대학교 대학원 치의공학과

(지도교수: 김 홍 중)

최근의 연구에 의하면 생쥐에서 *Nfic*가 결손 되면 구치 치근의 발생이 잘 이루어지지 않고 심각한 절치의 변형이 나타나는 것으로 알려지고 있다. *Nfic*의 결손은 상아모세포의 분화 이상을 일으켜서 결과적으로 비정상적인 상아질 형성을 유도하나, 법랑모세포를 포함하는 신체의 다른 세포들의 이상은 유발하지 않는다. 이들 결과에 기초하여 이 연구에서는 상아모세포에서 *Nfic*의 기능을 구명하고자 하였다.

생후 10일과 18일의 정상과 *Nfic* 결손 생쥐의 치아표본에서 형태학적인 관찰을 하였고, 일차치수세포와 MDPC-23 세포를 사용하여 분자생물학적인 분석을 시행하였다.

Nfic 결손 생쥐에서 변성된 상아모세포들이 상아질과 유사한 석회화 조직에 함입되어 나타났다. 비정상적인 상아모세포는 강한 BSP의 발현을 보였으며 정상과 비교하여 낮은 DSPP의 발현을 보였다. *Nfic* 유전자 결손은 변성된 상아모세포와 치수세포에서 p-Smad2/3의 증가를 보였다. 세포의 증식능 분석에서는 *Nfic* 결손 생쥐의 치경륜 부위에서 정상과 비교하여 세포 증식력의 감소를 보였다. 부가적으로 *Nfic* 결손 치수세포에서 p21의 증가와 cyclin D1과 B1의 감소를 보였는데 이는 *Nfic*의 활성 저하에 기인한 세포의 성장억제를 암시한다. *Nfic* 결손 생쥐 치수세포의 세포사멸 분석에서는 사멸활성의 증가와 caspase-8과 -3의 활성 증가를 보였다.

위의 결과들을 종합하면 *Nfic*의 결손은 상아모세포의 증식과 분화를 억제하며 치근형성 동안에 변성된 상아모세포의 사멸을 유도하여 짧은 치근의 형성에 관여하는 것으로 생각된다.

저작물 이용 허락서

학 과	치의공학과	학 번	20077438	과 정	박사
성 명	한글: 김지웅 한문 :		영문: Kim, Ji-Woong		
주 소	302-120 대전 서구 둔산동 1509 크로바아파트 104-1309				
연락처	E-MAIL :				
논문제목	한글 : *Nfic* 유전자 결손이 상아모세포 분화와 상아질 형성에 미치는 영향				
	영문: Effect of *Nfic* disruption on odontoblast differentiation and dentin formation				

본인이 저작한 위의 저작물에 대하여 다음과 같은 조건아래 조선대학교가 저작물을 이용할 수 있도록 허락하고 동의합니다.

- 다 음 -

1. 저작물의 DB구축 및 인터넷을 포함한 정보통신망에의 공개를 위한 저작물의 복제, 기억장치에의 저장, 전송 등을 허락함
2. 위의 목적을 위하여 필요한 범위 내에서의 편집·형식상의 변경을 허락함. 다만, 저작물의 내용변경은 금지함.
3. 배포·전송된 저작물의 영리적 목적을 위한 복제, 저장, 전송 등은 금지함.
4. 저작물에 대한 이용기간은 5년으로 하고, 기간종료 3개월 이내에 별도의 의사 표시가 없을 경우에는 저작물의 이용기간을 계속 연장함.
5. 해당 저작물의 저작권을 타인에게 양도하거나 또는 출판을 허락을 하였을 경우에는 1개월 이내에 대학에 이를 통보함.
6. 조선대학교는 저작물의 이용허락 이후 해당 저작물로 인하여 발생하는 타인에 의한 권리 침해에 대하여 일체의 법적 책임을 지지 않음
7. 소속대학의 협정기관에 저작물의 제공 및 인터넷 등 정보통신망을 이용한 저작물의 전송·출력을 허락함.

동의여부 : 동의(V) 반대( )

2009년 2월 일

저작자: 김 지 웅 (서명 또는 인)

조선대학교 총장 귀하